Proceedings of the 2007 IEEE/RSJ International
Conference on Intelligent Robots and Systems
San Diego, CA, USA, Oct 29 - Nov 2, 2007

Wheeled Inverted Pendulum Type Assistant Robot: Inverted Mobile, Standing, and Sitting Motions

SeongHee Jeong and Takayuki Takahashi

Abstract— **This paper describes the mobile control and the standing and sitting motions of an Inverted PENdulum Type Assistant Robot-(I-PENTAR) aiming at the coexistence of safety and work capability. I-PENTAR consists of a body with a high powered waist joint, arms designed for safety, and a wheeled inverted pendulum mobile platform. It is modeled as a three-dimensional robot with controls for inclination angle, linear position, and steering angle, and is controlled by state feedback control based on the LQR method. The motion planning of standing and sitting-important motions for an inverted pendulum type robot in practical use-is proposed. It was experimentally confirmed that I-PENTAR could realize a series of fundamental motions required in practical use, which are standing, running, turning, and sitting stably.**

I. Introduction

A. Background

Recently, many robots have been developed for providing physical assistance to humans in various activities such as delivery and cleaning. It is essential that robots with high work capability provide not only various services but also high safety without causing any injury. However, since the two functions possess characters that mutually conflict with each other, it is difficult to reconcile them. For example, although safety is usually realized by making a lightweight, low speed, and low-power robot, this will cause a drop in its working capabilities such as loading and movement.

A robot with an inverted pendulum mobile platform provides an effective solution to this problem. Since the robot always tries to keep its balance using the information on the center of gravity(CoG), it is able to perform work that demands high power with a low power and lightweight arm by employing its self-weight. In addition, the robot has some useful characteristics as a human assistant robot. First, since it has a simpler structure, it contributes to reducing the weight of the system compared to a bipedal robot. Second, it ensures high safety against overturn when unpredictable collision occurs, because it is always controlled to maintain dynamic stability. Finally, since it has a mechanically small footprint and does not have any caster, it can achieve high mobility such as quick response and high traveling ability on a bump. From these features, a two-wheeled inverted pendulum type robot can be considered greatly suitable for supporting human work that requires high safety and work capability.

B. Related research

Many studies on the wheeled inverted pendulum type robot focus on improving its mobility, such as running, steering, and trajectory following. Yamafuji [1] [2] [3] proposed a wheeled inverted pendulum type robot and realized stable traveling with it; Matumoto [4] [5] examined stable travel of the robot by estimating its attitude using only internal sensors on a flat road as well as on an inclined path. Ha and Yuta [7] [8] developed an inverted pendulum mobile robot that could traverse an indoor environment with high mobility and robustness. Although the robots in the above-mentioned studies were modeled as two-dimensional robots, certain studies have modeled them as three-dimensional ones in order to simultaneously perform balancing, linear running, and steering control [9] [10] [12] [14].

On the other hand, a few studies have been conducted to realize not only the movements but also the tasks of the robot. Matumoto [6] realized a cooperative transportation task between two wheeled inverted pendulum robots by estimating the external force and the acting force by an observer. Bryan [15] recently proposed a pushing task that uses the robot's dynamic stability.

C. Research target

As shown above, most studies on the wheeled inverted pendulum robot focus on its balancing stability and mobility, and few studies consider its work capability as a human assistant robot. The aim of this study is to develop an assistant robot with high safety and work capability by employing a wheeled inverted pendulum mechanism, and to realize various motions, such as standing and sitting, picking up an object from the ground, and lifting a heavy object. In this paper, we briefly describe the proposed robot Inverted PENdulum Type Assistant Robot-(I-PENTAR)-, and focus on the realization of inverted mobile, standing, and sitting motions, which are the fundamental motions of a human assistant robot. In particular, the standing and sitting motions are considered as essential motions for an inverted pendulum type assistant robot to be a practical one, which frequently changes from a static to a dynamic stable state.

II. Inverted Pendulum Type Assistant Robot

Figure 1 shows the appearance of the prototype robot proposed in this study, I-PENTAR, and Table I describes the general specifications of the robot. To realize various functions, I-PENTAR is composed of a body with a waist joint, two low-powered and light arms, and a two-wheeled inverted pendulum type mobile platform.

It adopts a double motor method for its mobile platform, which actuates a wheel with two motors-in order to reduce the effect of backlash in balancing control and to increase the power of the mobile platform. The lower body shares

1-4244-0912-8/07/$25.00 ©2007 IEEE.

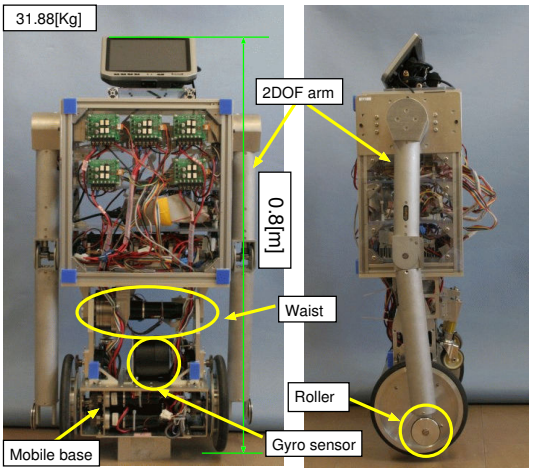

Fig. 1. Proposed inverted pendulum type assistant Robot, I-PENTAR

TABLE I
GENERAL SPECIFICATIONS OF I-PENATR

Size	[m]	900 [H] × 340 [W] × 210 [D]
Weight	[kg]	32
DOF		Mobile (2), Arm (4), Waist (1)
CPU		Pentium3 500 [Mhz]
Sensor		Gyro sensor(1), Encoder(9)
OS		ARTLinux(Sampling time:1 [ms])

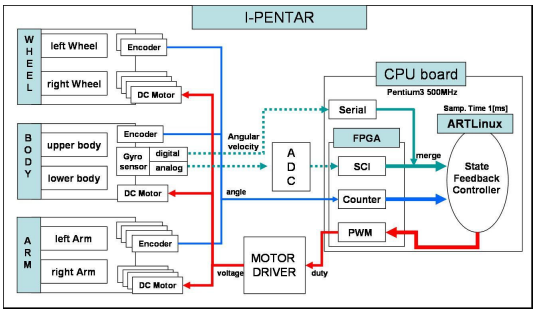

Fig. 2. Internal signal flow of I-PENTAR

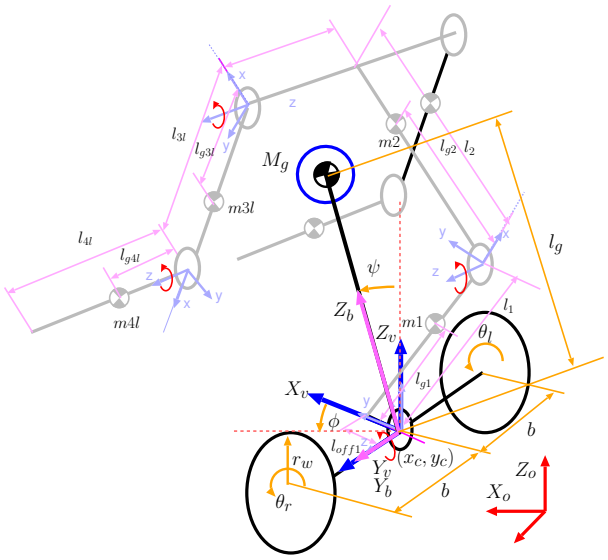

Fig. 3. Model of 3DOF wheeled inverted pendulum robot

its axis with the wheel and freely rotates about its axis, thereby realizing an inverted pendulum mechanism. The body is divided into lower and upper parts by a waist joint, which adopts a harmonic gear to reduce any backlash, and a rate gyro sensor is located in the lower body to detect the inclination angle with respect to the ground. An mechanical stopper is placed at the elbow to execute a task that requires high power even when a high-power actuator is not present. In addition, a wheel type roller adheres to the tip of the arm to push the body up and down by sliding it during standing and sitting motions. The internal signal flow of I-PENTAR is depicted in Fig.2. The control and sensor signals between each part and a CPU board are interfaced via an FPGA board in 1 [ms] sampling time. The two angular velocity values, analog and digital, obtained from the rate gyro sensor are merged and integrated to be used for the inclination angle of the lower body.

III. MOBILE CONTROL

A. Modeling

As mentioned before, in most studies, a wheeled inverted pendulum robot is built as a two-dimensional model with an inclination angle and a linear position. In this case, since the dynamics due to the steering motion is not considered in the model, the robot becomes unstable while running along a curve at high speed. For this reason, in this study, I-PENTAR is built as a three-dimensional model by including a steering angle in the two-dimensional model.

The model of I-PENTAR for mobile control is shown in Fig. 3. It has two wheels and a body that includes all parts except the wheels; therefore, the CoG in the model represents the composite center of gravity (CCoG) of the whole robot excluding the wheels. The origin of vehicle coordinates Σ_v is located at the midpoint on the line that connects the axis of the two wheels, and the origin of the body coordinates Σ_b coincides with Σ_v. The angle between z_b and z_v represents the inclination angle of the body ψ, and the angle between x_v and X_o axis of the global coordinates represents the steering angle ϕ. In all coordinates, counterclockwise(CCW) direction is positive. The parameters of the model are presented in Table II.

B. 3DOF motion equations

In this section, the motion equations of I-PENTAR for mobile control is derived. Defining a generalized coordinate as $(x_c, y_c, \phi, \psi, \theta_r, \theta_l)$, the motion equation of the robot is derived using the Lagrange equation with constraints as

$$\boldsymbol{M(q)\ddot{q} + H(q,\dot{q}) + V\dot{q} + G = E\tau + A(q)^T\lambda} \quad (1)$$

where $\boldsymbol{M(q)} \in R^{6\times6}$ is an inertia matrix, $\boldsymbol{H(q,\dot{q})} \in R^{6\times1}$ is coliori and centrifugal force, $\boldsymbol{V} \in R^{6\times1}$ is a viscous coefficient matrix, $\boldsymbol{G} \in R^{6\times1}$ is gravity force, $\boldsymbol{E\tau} \in R^{6\times1}$ is control torque, $\boldsymbol{A(q)}$ is a matrix that represents the

TABLE II

ROBOT PARAMETERS

θ_r, θ_l	[rad]	Rotational angle of the wheel
x_c, y_c	[m]	Position of the vehicle in Σ_o
ψ	[rad]	Inclination angle of CoG
ϕ	[rad]	Steering angle of the vehicle
M_g	[Kg]	Mass of CCoG
m_w	[Kg]	Mass of the wheel
l_g	[m]	Length between vehicle's origin and CoG
b	[m]	Distance between vehicle's origin and wheel's origin
r_w	[m]	Radius of the wheel
$\boldsymbol{I}_g$	[Kgm^2]	Body's inertia
I_{wa}	[Kgm^2]	Wheel's inertia (axis)
I_{wd}	[Kgm^2]	Wheel's inertia (diameter)
I_{ra}	[Kgm^2]	Motor rotor's inertia (axis)
I_{rd}	[Kgm^2]	Motor rotor's inertia (diameter)
c_r, c_l	[Nm/(rad/s)]	Viscosity coeff. of the wheel

constraints of the robot, and $\boldsymbol{\lambda}$ is a Lagrange multiplier. In order to derive $\boldsymbol{A}(\boldsymbol{q})$, let us consider the constraints of a two-wheeled mobile robot. Generally, there are three constraints in the robot, assuming that the wheels do not slip, which are given as

$$\dot{x}_c \sin\phi - \dot{y}_c \cos\phi = 0 \quad (2)$$

$$\dot{x}_c \cos\phi + \dot{y}_c \sin\phi = \frac{r_w}{2}(\dot{\theta}_r + \dot{\theta}_l) \quad (3)$$

$$\dot{\phi} = \frac{r_w}{2b}(\dot{\theta}_r - \dot{\theta}_l) \quad (4)$$

Here, (2) and (3) are non-holonomic constraints and (4) is a holonomic one. These equations are then expressed as the following:

$$\boldsymbol{A}(\boldsymbol{q})\dot{\boldsymbol{q}} = \boldsymbol{0} \quad (5)$$

where

$$\boldsymbol{A}(\boldsymbol{q}) = \begin{bmatrix} \sin\phi & -\cos\phi & 0 & 0 & 0 & 0 \\ \cos\phi & \sin\phi & b & 0 & -r_w & 0 \\ \cos\phi & \sin\phi & -b & 0 & 0 & -r_w \end{bmatrix}$$

Here, we define a matrix $\boldsymbol{S}(\boldsymbol{q})$, which is composed of linear independent vector in the null-space of $\boldsymbol{A}(\boldsymbol{q})$ as given below.

$$\boldsymbol{S}(\boldsymbol{q}) = \begin{bmatrix} \cos\phi & 0 & 0 \\ \sin\phi & 0 & 0 \\ 0 & 1 & 0 \\ 0 & 0 & 1 \\ 1/r_w & b/r_w & 0 \\ 1/r_w & -b/r_w & 0 \end{bmatrix} \quad (6)$$

In this case, $\boldsymbol{A}(\boldsymbol{q})\boldsymbol{S}(\boldsymbol{q}) = \boldsymbol{0}$ since $\boldsymbol{S}(\boldsymbol{q})$ is included in the null-space of $\boldsymbol{A}(\boldsymbol{q})$. Moreover, since $\dot{\boldsymbol{q}}$ always exists in the null-space of $\boldsymbol{A}(\boldsymbol{q})$, defining a new velocity vector $\boldsymbol{\nu} = [v\ \dot{\phi}\ \dot{\psi}\ ]$, the following equations are satisfied.

$$\dot{\boldsymbol{q}} = \boldsymbol{S}(\boldsymbol{q})\boldsymbol{\nu} \quad (7)$$

$$\ddot{\boldsymbol{q}} = \dot{\boldsymbol{S}}(\boldsymbol{q})\boldsymbol{\nu} + \boldsymbol{S}(\boldsymbol{q})\dot{\boldsymbol{\nu}} \quad (8)$$

Consequently, substituting (7) and (8) in (1) and rearranging it, we obtain

$$\hat{\boldsymbol{M}}\dot{\boldsymbol{\nu}} + \hat{\boldsymbol{H}}(\boldsymbol{\nu}, \dot{\boldsymbol{\nu}}) + \hat{\boldsymbol{V}}\boldsymbol{\nu} + \hat{\boldsymbol{G}} = \hat{\boldsymbol{E}}\boldsymbol{\tau} \quad (9)$$

where $\hat{\boldsymbol{M}} = \boldsymbol{S}(\boldsymbol{q})^T\boldsymbol{M}(\boldsymbol{q})\boldsymbol{S}(\boldsymbol{q})$, $\hat{\boldsymbol{H}} = \boldsymbol{S}(\boldsymbol{q})^T[\boldsymbol{M}(\boldsymbol{q})\dot{\boldsymbol{S}}(\boldsymbol{q})\boldsymbol{\nu} + \boldsymbol{H}(\boldsymbol{q}, \dot{\boldsymbol{q}})]$, $\hat{\boldsymbol{V}} = \boldsymbol{S}(\boldsymbol{q})^T\boldsymbol{V}\boldsymbol{S}(\boldsymbol{q})$, $\hat{\boldsymbol{G}} = \boldsymbol{S}(\boldsymbol{q})^T\boldsymbol{G}$, and $\hat{\boldsymbol{E}} = \boldsymbol{S}(\boldsymbol{q})^T\boldsymbol{E}$. These equations represent the motion equations of the robot considering the holonomic and non-holonomic constraints.

C. Inverted mobile motion

For the inverted mobile motion of I-PENTAR, in this study, we adopt a state feedback control method and decide the feedback gain in the controller by the LQR(Linear Quadratic Regulator) method. In order to use the control method, first, (9) should be linearized since it is nonlinear. Apart from the generalized coordinate used in the motion equation, a new generalized coordinate, $\boldsymbol{q}_\nu = [x\ \phi\ \psi]$, is introduced as an actual control variable. Then, the state variables in the system can be represented as $\boldsymbol{x} = [\boldsymbol{q}_\nu\ \boldsymbol{\nu}]$. To linearize the system, it is approximated to around $\boldsymbol{x} \cong \boldsymbol{0}$. Accordingly, in (9), $\hat{\boldsymbol{H}}$ disappears, and the equation can be simplified as

$$\hat{\boldsymbol{M}}\dot{\boldsymbol{\nu}} + \hat{\boldsymbol{V}}\boldsymbol{\nu} + \hat{\boldsymbol{G}} = \hat{\boldsymbol{E}}\boldsymbol{\tau} \quad (10)$$

where $\hat{\boldsymbol{M}}$ and $\hat{\boldsymbol{G}}$ are the linearized values. Therefore, the linearized state equation of the system is given as

$$\begin{aligned} \dot{\boldsymbol{q}}_{\boldsymbol{\nu}} &= \boldsymbol{\nu} \\ \dot{\boldsymbol{\nu}} &= -\hat{\boldsymbol{M}}^{-1}(\hat{\boldsymbol{V}}\boldsymbol{\nu} + \hat{\boldsymbol{G}}) + \hat{\boldsymbol{M}}^{-1}\hat{\boldsymbol{E}}\boldsymbol{\tau} \end{aligned}$$

$$\dot{\boldsymbol{x}} = \boldsymbol{A}\boldsymbol{x} + \boldsymbol{B}\boldsymbol{u} \quad (11)$$

$$\boldsymbol{A} = \begin{bmatrix} 0 & 0 & 0 & 1 & 0 & 0 \\ 0 & 0 & 0 & 0 & 1 & 0 \\ 0 & 0 & 0 & 0 & 0 & 1 \\ 0 & 0 & a_{43} & a_{44} & a_{45} & a_{46} \\ 0 & 0 & 0 & a_{54} & a_{55} & a_{56} \\ 0 & 0 & a_{63} & a_{64} & a_{65} & a_{66} \end{bmatrix} \boldsymbol{B} = \begin{bmatrix} 0 & 0 \\ 0 & 0 \\ 0 & 0 \\ b_1 & b_2 \\ b_3 & b_4 \\ b_5 & b_6 \end{bmatrix}$$

where $a_{43} = \frac{M_g^2 l_g^2 r_w^2 G}{V_1}$, $a_{44} = \frac{w_1 c_1}{V_1}$, $a_{45} = \frac{b w_1 c_2}{V_1}$, $a_{46} = -\frac{r_w w_1 c_1}{V_1}$, $a_{54} = -\frac{b c_2}{V_2}$, $a_{55} = -\frac{b^2 c_1}{V_2}$, $a_{56} = \frac{b r_w c_2}{V_2}$, $a_{63} = -\frac{(M_g r_w^2 + 2m_w r_w^2 + 2(I_{wa} + I_{ra}\gamma^2))M_g l_g G}{V1}$, $a_{64} = -\frac{w_2 c_1}{r_w V_1}$, $a_{65} = -\frac{b w_2 c_2}{r_w V_1}$, $a_{66} = \frac{w_2 c_1}{V_1}$,
$b_1 = b_2 = -\frac{r_w w_1}{V_1}$, $b_3 = -b_4 = \frac{r_w b}{V_2}$, $b_5 = b_6 = \frac{w_2}{V_1}$,
$V_1 = M_g^2 l_g^2 r_w^2 - (M_g l_g^2 + I_{yy}) M_g r_w^2 - 2(M_g l_g^2 + I_{yy}) m_w r_w^2 - 2(M_g l_g^2 + I_{yy})(I_{wa} + I_{ra}\gamma^2)$,
$V_2 = I_{zz} r_w^2 + 2(I_{wd} + I_{rd}) r_w^2 + 2m_w r_w^2 b^2 + 2(I_{wa} + I_{ra}\gamma^2) b^2$,
$w_1 = M_g l_g^2 + I_{yy} + M_g l_g r_w$, $w_2 = M_g l_g r_w + M_g r_w^2 + 2m_w r_w^2 + 2(I_{wa} + I_{ra}\gamma^2)$, and $c_1 = c_r + c_l$, $c_2 = c_r - c_l$.

The evaluation function of LQR is generally given as

$$J = \frac{1}{2}\int_0^a (\boldsymbol{x}^T\boldsymbol{Q}\boldsymbol{x} + \boldsymbol{u}^T\boldsymbol{R}\boldsymbol{u})dt \quad (12)$$

and the control input that minimizes the function is

$$\boldsymbol{u} = -\boldsymbol{K}\boldsymbol{x} \quad (13)$$

By inputting $\boldsymbol{u}$ to the wheel motors, I-PENTAR can run and steer while maintaining its balance.

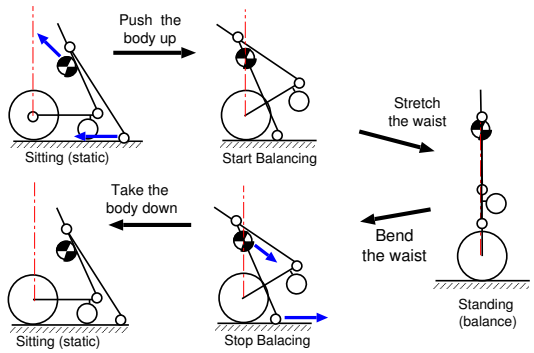

Fig. 4. A series of standing and sitting motions

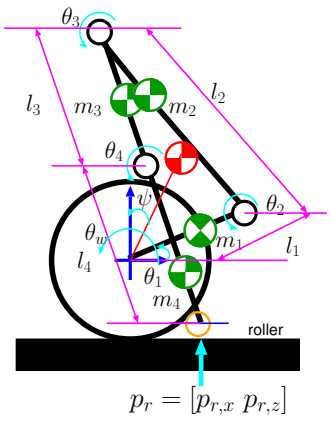

Fig. 5. Four-link model of I-PENTAR for standing and sitting motion

IV. Standing and Sitting Motion

It is desirable for a human assistant robot to be able to perform functions both in static and dynamic stable states. I-PENTAR is designed to cope with the requirements. In this chapter, the standing and sitting motion planning of I-PENTAR which changes its state from static to dynamic stable or vice versa, is described.

A. Overall motion strategy

A series of standing and sitting motions is shown in Fig. 4. The robot is initially in a static stable state. In standing motion, it is pushed up by two arms until its CCoG is located above the wheel axle, and then begins balancing control to achieve dynamic stability. Then, it stretches the waist until an upright-standing posture is achieved. In sitting motion, the robot bends the waist while maintaining its balance until the roller reaches right above the ground. Next, it turns off the balancing control in order to ground the roller and slides it in the backward direction to achieve a static stable posture.

The four-link model of the robot for standing and sitting motions is shown in Fig. 5. The six variables in the model are the angle of the wheel θ_w, the inclination angle of the body ψ, and the joint angle of each link $\theta_1, \theta_2, \theta_3, and \theta_4$. Among them, ψ and θ_1 are the variables that cannot be directly moved by an actuator while other variables can be moved. Therefore, the standing and sitting motions shown in Fig. 4 present the problem of how to control these variables. In the following section, the motion planning of standing and sitting is described in detail.

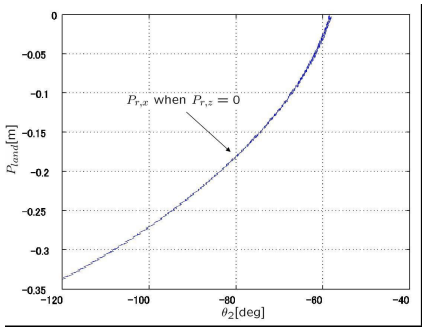

Fig. 6. Attainable landing position of the roller

B. Standing motion

It is relatively easy to achieve standing motion compared to sitting motion. Initially, the robot is in a static stable state so that its CCoG is located inside the polygon formed by two wheels and casters. When the standing motion begins, the robot rotates the shoulder joint θ_3 in the clockwise(CW) direction with θ_w fixed, so that the CCoG is pushed up and the inclination angle of the body ψ increases. During the motion, the hinge angle θ_4 is fixed to cope with high bending torque applied to it. When ψ becomes zero, the balancing control begins to achieve dynamic stability. The roller should be quickly moved away from the ground so that it is not in contact with the ground after the balancing control begins. Finally, the robot begins to rotate the waist angle θ_2 until the upright-standing posture is achieved while maintaining dynamic stability, which means that ψ = 0. In this case, θ_1 is automatically decided according to the posture of the whole body.

C. Sitting motion

Sitting motion can be realized by following the reverse process of the standing motion. The robot bends its waist θ_2 in the CCW direction from the upright-standing posture while maintaining ψ=0. When the position of the roller's tip P_z is close to the ground, balance control is stopped and the robot achieves the static stable state by the supporting points of the wheel and the roller. There are two conditions that should be considered while executing this motion. The first is the selection of a landing point of the roller P_{land}. While selection P_{land}, it is necessary to consider that the roller can reach the ground in the movable range of θ_2. This is because a high impact force is exerted on the roller when the balancing control is stopped and the roller is not in contact with the ground despite the limitation of θ_2. Moreover, P_{land} should be behind the wheel axle, because the robot may overturn when the roller slides forward and backward.

Figure 6 shows the attainable landing point P_{land} in the movable range of θ_2. By selecting the landing point from the figure, the robot can realize sitting motion without causing a failure. The second is the switching time of the balancing

TABLE III

PARAMETERS OF I-PENTAR

M_g	[Kg]	25.26
m_w	[Kg]	1.25 × 2
l_g	[m]	0.4005
b	[m]	0.16
r_w	[m]	0.1
$\boldsymbol{I}_g$	[Kgm^2]	(1.408,1.39,0.1082)
I_{wa}	[Kgm^2]	0.01475
I_{wd}	[Kgm^2]	0.0073
I_{ra}	[Kgm^2]	0
I_{rd}	[Kgm^2]	0
γ		1
c_r, c_l	[Nm/(rad/s)]	(0.1, 0.1)
G	[m/s^2]	9.81

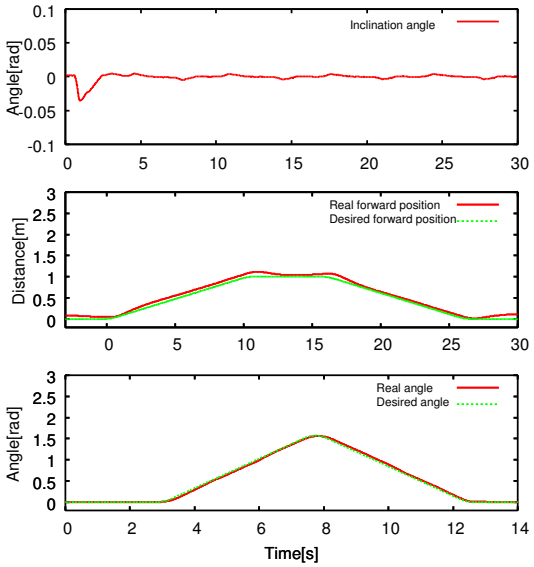

Fig. 7. Experimental result of mobile motion

control. Balancing control should be stopped when ψ has a negative value; otherwise, the robot will fall forward. To obtain a negative value of ψ, the robot should be accelerated backward before balancing is stopped. By doing this, forward falling can be avoided. After landing the roller, the robot rotates the shoulder joint θ_3 in the CW direction and, finally, makes its casters contact the ground.

V. EXPERIMENT

Several experiments are conducted with I-PENTAR to evaluate the proposed mobile control method and the standing and sitting motion planning. The optimal gain $\boldsymbol{K}$ can be obtained from the parameter values in Table III using MATLAB as

$$\boldsymbol{K} = \begin{bmatrix} -22 & 22 & -114 & -25 & 3 & -20 \\ -22 & -22 & -114 & -25 & -3 & -20 \end{bmatrix} \quad (14)$$

where $\boldsymbol{Q}$ is diag([100 100 1000 0.1 0.1 0.1]) and $\boldsymbol{R}$ is diag([0.1 0.1]).

A. Inverted mobile motion

Balancing, linear running, and steering experiments are conducted. In these experiments, I-PENTAR takes an upright-standing posture by stretching its waist and extending the two arms toward the ground.

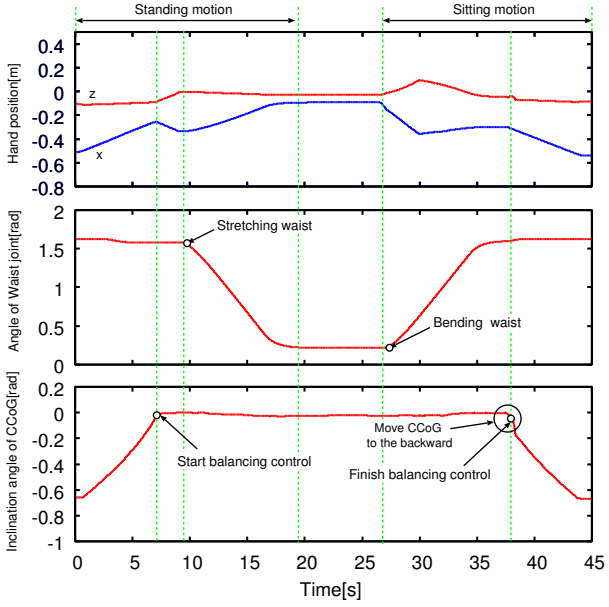

Fig. 8. Experiment results of standing and sitting motion

1) Balancing control: In the balancing experiment, I-PENTAR keeps its balance initially and is pushed by an arbitrary force from the back. Figure 7 (top) shows the inclination angle of CCoG in the experiment. From the figure, we can infer that the body of I-PENTAR inclines backward because of the force and returns to the original state after the force is removed, and then, maintains its balance.

2) Linear running control: Figure 7 (middle) shows the displacement of the robot in the linear running experiment. In this experiment, a troplized-type velocity trajectory is given; the goal acceleration, velocity, and position are 0.2 [$\mathbf{m/s^2}$], 0.1 [m/s], and 1 [m], respectively. From the figure, it is confirmed that the robot follows its desired trajectory well.

3) Steering control: In the steering experiment, the robot is operated so that it is rotated in the CCW direction on a spot. Figure 7 (bottom) shows the profile of the steering angle in the experiment. From the figure, it can be inferred that the rotation angle of the robot follows desired steering angle.

B. Standing and sitting motion

In this experiment, I-PENTAR achieves the posture by bending its waist and grounding the rollers, where $(\theta_1, \theta_2, \theta_3, \theta_4)$ are $(-87,\ 110,\ 200,\ 5)$ [deg]. During the experiment, θ_4 (hinge joint) is fixed as 5 [deg].

Figure 8 shows the position of the roller's tip P_r (top), the angle of the waist joint θ_2 (middle), and the inclination angle of CCoG ϕ (bottom). The inclination angle of CCoG in the initial state is -36 [deg], and therefore, CCoG is located inside the supporting points formed by the wheels and casters. When the standing motion begins, the rollers slide toward the positive direction of x, and the balancing

Fig. 9. Video clips of standing, inverted mobile, and sitting motion of I-PENTAR

control begins when ψ is -2 [deg] wherein $P_{r,x}$ is -0.32 [m]. Then, the robot rotates its waist by 10 [deg/s] in the CW direction until the angle becomes 10 [deg] while maintaining ψ at around 0 [deg] and then finishes the standing motion. In the sitting motion, it bends the waist and makes the rollers approach the ground. During this motion, $P_{r,x}$ is maintained at -0.32 [m]. When the position of the roller's tip $P_{r,z}$ becomes -0.09 [m], the robot inclines its CCoG backward and the balancing control is stopped, so that it becomes stable with support from the wheels and the rollers. Then, it further slides the rollers backward until $P_{r,x}$ becomes -0.5 [m] and makes the casters contact the ground.

Some video clips of standing, inverted mobile, and sitting motion of I-PENTAR are shown in Fig.9.

VI. Conclusion

In this paper, a human assistant robot, I-PENTAR, which aims at achieving both high safety and work capability, is proposed, and its inverted mobile, standing, and sitting motions are described. In the inverted mobile control, the balancing, linear running, and steering control were performed using a state feedback controller, and it is confirmed through experiments that these motions can be achieved stably. The standing and sitting motion planning was preformed and its effectiveness was confirmed through an experiment. As a future work, we will consider the dynamic effect of the robot in a mobile control to achieve agiler motion, and realize more dexterous standing and sitting motions.

References

[1] Kazuo Yamafuji, Takashi Kawamura,"Postural Control of a Monoaxial Bicycle", JRSJ, Vol 7, no.4, pp 74-79, 1988.

[2] Kazuo Yamafuji, Yasushi Miyakawa, Takashi Kawamura, "Synchronous Steering Control of a Parallel Bicycle", JSME, vol. 55, no.513, pp.1229-1234, 1989.

[3] Tsuyoshi Yasui, Kazuo Yamafuji, "Motion control of the Parallel Bicycle-Type Mobile Robot which is composed of a Triple Inverted pendulum(1st Report, Stability Control of Standing Upright, Ascending and Descending of Stairs", JSME, Vol.57(C), no.538, pp 114-119, 1991.

[4] Osamu Matsumoto, Shuuji Kajita, Kazuo Tani, "Estimation and Control of Attitude of a Dynamic Mobile Robot Using Internal Sensors", JRSJ, Vol. 8, no. 5, pp 37-46, 1990.

[5] Osamu Maisumoto, Shuuji Kajita, kazuo Tani, "Attitude Estimation of the Wheeled Inverted Pendulum Using Adaptive Observer", 19th Annual Conference of RSJ, pp 909-910, 1991.

[6] Osamu Maisumoto, Shuuji Kajita, kazuo Tani, "Cooperative Behavior of a Mechanically Unstable Mobile Robot for Object Transportation", JSME, Vol.64(C), no. 628, pp 164-171, 1998.

[7] Yunsu Ha, Shinichi Yuta, "Trajectory Tracking Control for Navigation of Self-Contained Mobile Inverse Pendulum", Proc. of the 1994 IEEE/RSJ int. Conf. on Intelligent Robotics and Systems, pp.1875-1882, 1994.

[8] Yunsu Ha, Shinichi Yuta, "Indoor Navigation of an Inverse Pendulum Type Autonomous Mobile Robot with Adaptive Stabilization Control System", 4th International Symposium on Experimental Robotics (ISER) '95 pp.331-336 1995-06.

[9] Felix Grasser, Aldo D'Arrigo, Silvio Colombi, "JOE: A Mobile, Inverted Pendulum", IEEE Trans. on Industrial Electronics, Vol. 49, no. 1, 2002.

[10] Kaustubh Pathak, Jaume franch, Sunil K. Agrawal, "Velocity Control of a Wheeled Inverted Pendulum by Partial Feedback Linearization", IEEE Conference on Decision and Control, pp 3962-3967, 2004.

[11] Kaustubh Pathak, Jaume franch, Sunil K. Agrawal, "Velocity and Position Control of a Wheeled Inverted Pendulum by Partial Feedback Linearization", IEEE Trans. on Robotics, Vol. 21, no.3, pp 505-512, 2005.

[12] Yeon Hoon Kim, Dong-Yeon Lee, Soo Hyun Kim, Yoon Keun Kwak, "Emotional Action Simulation of 2 Wheeled Inverted Pendulum Mobile Robot", The IASTED Conference on Modeling, Simulation, and Optimization, pp 266-271, 2003.

[13] Y Kim, S H Kim, and Y K Kwak, "Improving driving ability for a two-wheeled inverted-pendulum-type autonomous vehicle", Proc. of the Institution of Mechanical Engineers, Part D: Journal of Automobile Engineering, Vol.220, no.2, pp. 165 - 175, 2005.

[14] Michael Baloh, Michael Parent, " Modeling and Model Verification of an Intelligent Self-Balancing Two-Wheeled Vehicle for an Autonomous Urban Transportation System", The Conference on Computational Intelligence, Robotics, and Autonomous Systems, pp 1-7, 2003.

[15] Bryan J.Thibodeau, Patrick Deegan, Roderic Grupen, "Static Analysis of Contact Forces With a Mobile Manipulator", Proc. ICRA, pp 4007-4012, 2006.